# Supplemental Information

Stem Cell Factor-Based Identification and Functional Properties of In Vitro-Selected Subpopulations of Malignant Mesothelioma Cells

Walter Blum, László Pecze, Emanuela Felley-Bosco, Licun Wu, Marc de Perrot, and Beat Schwaller

Supplemental Figure S1. Testing of efficiency of lentiviral transduction (eGFP(+) cells) with -SO and -SORE6 constructs also monitored by expression of NLS-mCherry; Expression levels of additional stemness markers in ZL55-SO^{high} and ZL55-SO^{low}, as well as in RN5-SO^{high} and RN5-SO^{low} cells (data related to Figure 1).
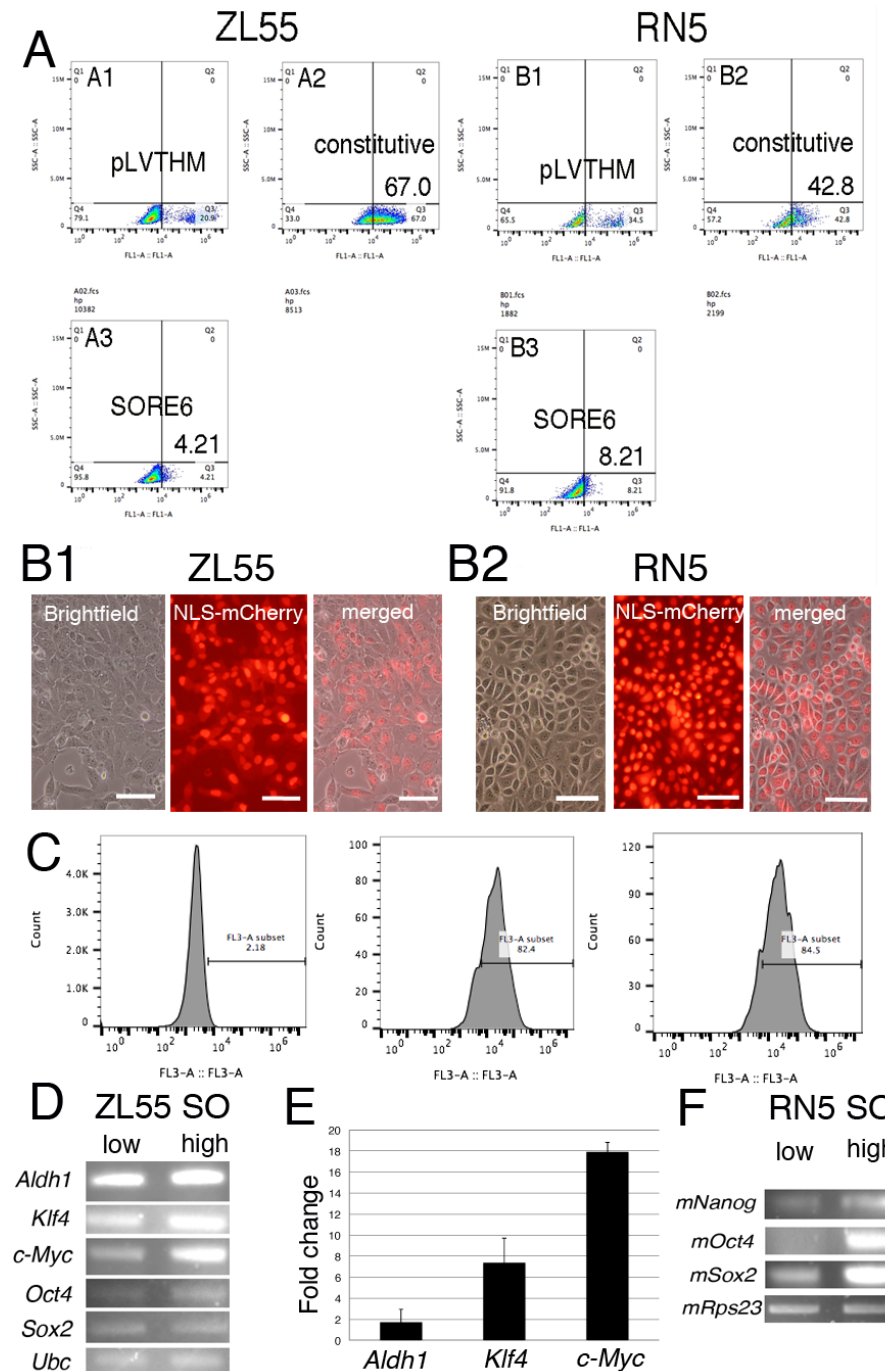
A) FACS analyses of eGFP expression in human ZL55 and mouse RN5 MM cells transduced with various lentiviruses. Lentivirus containing pLVTHM only (strong constitutive eGFP expression) was used to define the gating for eGFP(+) and eGFP(-) populations in ZL55 (A1) and RN5 (B1) cells. Cells transduced with the constitutive mCMVp-dsCopGFP-PURO construct (the same as the SORE6 construct, yet with a constitutively active CMV promoter) after puromycin selection for 48 h reveal a

high proportion of eGFP(+) cells. Note that the stringent gating was chosen to be very discriminative resulting in only 67% ZL55 cells identified as eGFP(+) (A2) and 42.8% of RN5 (B2) cells as eGFP(+). This ascertained that the number of false-positive cells is minimal. Under these conditions the percentage of eGFP(+) cells in ZL55 cells transduced with the SORE reporter construct SORE6-mCMVp-dsCopGFP-PURO (Tang et al., 2015) and selected with puromycin for 24 h is 4.21% for ZL55 cells (A3) and 8.21% for RN5 cells (A6). These values are almost identical to the ones observed after transduction with the Hotta construct (Hotta et al., 2009), i.e. 4.8% and 7.8%, respectively (Table 1). **B)** Brightfield (left image) and fluorescence (right image) images of ZL55 (B1) and RN5 (B2) cells transduced with a lentivirus coding for NLS-mCherry at a MOI of 10, previously shown to infect nearly all cells (Blum and Schwaller, 2013). **C)** FACS analysis of non-transduced RN5 cells (left panel; control), NLS-mCherry transduced cells RN5-SO^{low} cells (middle panel) and RN5-SO^{high} cells (right panel). The transduction rate is similar in RN5-SO^{low} and RN5-SO^{high} cells, 82.4% and 84.5% showed nuclear red fluorescence as reported by FACS, respectively. Scale bar: 100 µm. **D)** Semi-quantitative PCR of sorted ZL55-SO^{low} and ZL55-SO^{high} cells for previously reported additional putative cancer stem cell markers including *Aldh1*, *Klf4* and *c-Myc*. All bands are stronger in samples derived from RN5-SO^{high} cells; *Ubc* is used as the housekeeping gene and for the normalization in E). **E)** Quantitative RT-PCR analyses for the same markers reveal a 1.7 ± 1.2- fold increase for *Aldh1a1*, a 7.7 ± 2.3 -fold increase for *Klf4* and 17.9 ± 0.9-fold increase for *c-Myc* in the ZL55-SO^{high} cells compared to the ZL55-SO^{low} cells; error bars represent SEM from n= 3 independent experiments. **F)** Semi-quantitative PCR of RN5-SO^{low} and RN5-SO^{high} show an increase for *mNanog*, *mOct4* and *mSox2 in* RN5-SO^{high} cells; *mRps23* is used here as the housekeeping gene.

Supplemental Figure S2. Sorting of ZL55 and RN5 cells for eGFP(+) and eGFP(-) subpopulations sorting and monitoring of eGFP and determination of NLS-mCherry levels in cell cultures maintained for 45 days (data related to Figure 3).
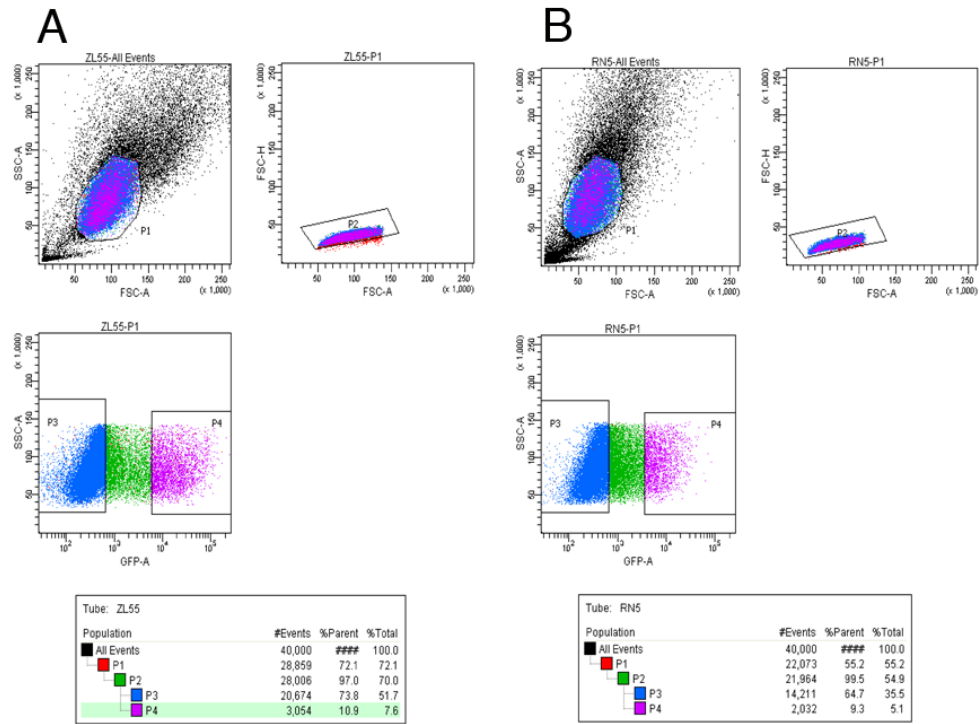

A) FACS sorting for ZL55-SO^{low} and ZL55-SO^{high} cells. Gatings were selected to obtain "pure" eGFP(+) cells (purple; population P4) and "pure" eGFP(-) cells (blue; population P3). **B)** The same approach was chosen to select mouse RN5-SO^{low} and RN5-SO^{high} cells.

Supplemental Figure S3. Increased tumorsphere forming (mesospheres) and colony-forming (anchorage-independent growth in soft agar) capacity of sorted –SO^{high} cells (data related to Fig. 4 & 5)
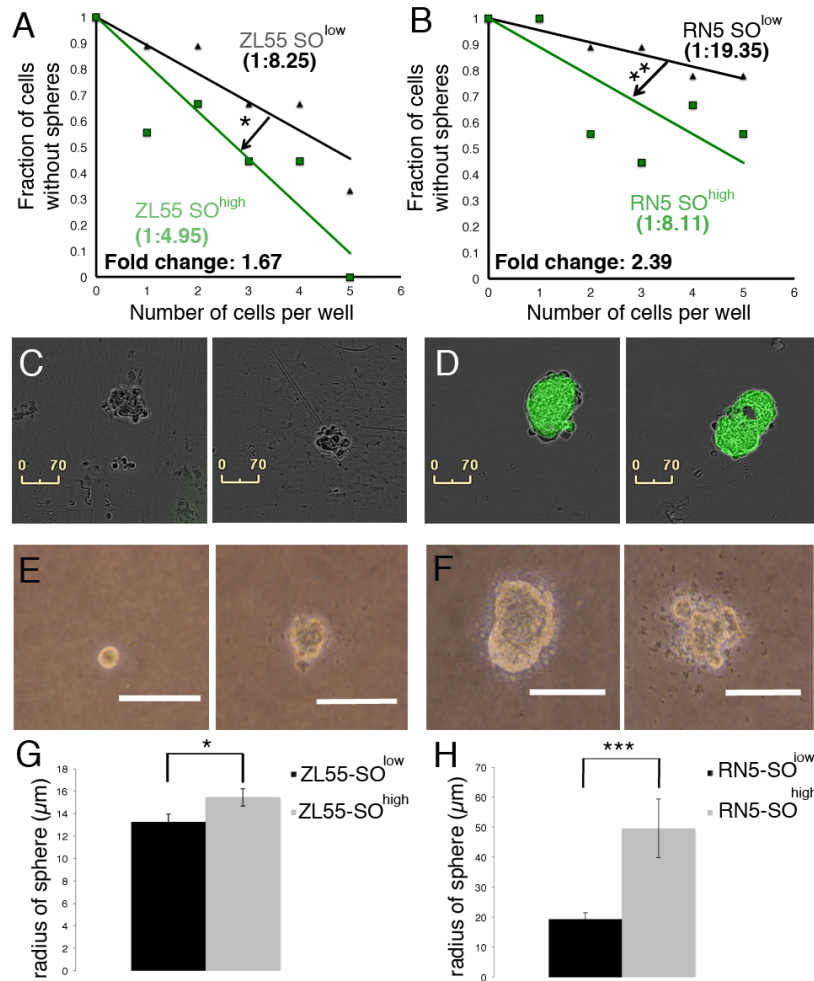
Limiting dilution assay *in vitro* with **A)** human ZL55-SO^{low} and ZL55-SO^{high} cells and **B)** with mouse RN5-SO^{low} and RN5-SO^{high} cells. The formation of spheres reported as "fraction of cells without spheres / number of cells per well" was evaluated after 10 days. A linear regression analysis of the slopes revealed significant differences between -SO^{high} eGFP(+) *vs*. -SO^{low} eGFP(-) cells for ZL55 (ANOVA *p < 0.05) and RN5 cells (**p < 0.005). Stem cell frequencies and fold change between eGFP(+) and eGFP(-) cells was calculated as described before (Thiagarajan et al., 2015). Representative images of tumorspheres from **C)** RN5-SO^{low} cells and from **D)** eGFP(+) RN5-SO^{high} cells. Scale bars: 70 µm. Representative colonies growing in soft agar (2 weeks) from **E)** RN5-SO^{low} cells and **F)** RN5-SO^{high} cells. Scale bars: 100 µm. The average sphere radius was calculated from randomly selected **G)** ZL55-SO (n=31 for both -SO^{low} and -SO^{high} cells) and **H)** RN5-SO (n=31 for -SO^{low} and n=13 for -SO^{high} cells). Results are from 3 independent experiments; values are mean±SEM; *p<0.05; ***p < 0.0005.

Supplemental Figure S4. Functional characterization of selected MM cells with respect to spheroid formation, mobility, non-directed movements and sensitivity towards NF2 up-regulation (data related to Figure 6).
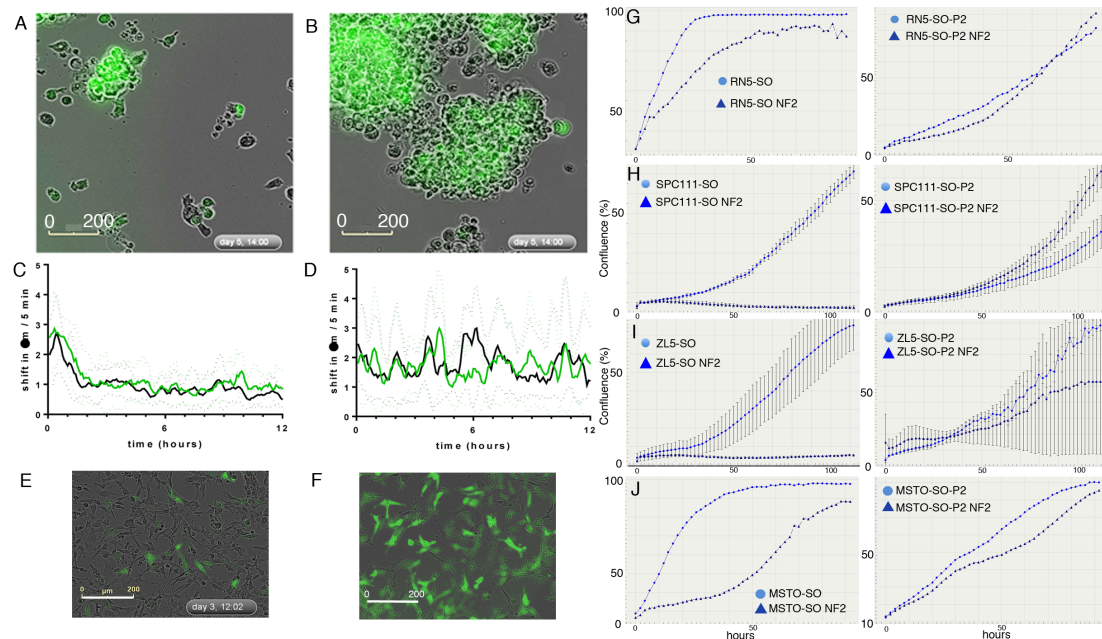
A) Spheroid-forming capacity of MSTO-211H-SO cells containing approximately 7% of eGFP(+) cells in the absence of serum. The percentage of eGFP(+) cells within spheroids is increased compared to regular 2D-cultures of MSTO-211H-SO cells (**A**). In the population of MSTO-211H-SO-P2 cells consisting largely of eGFP(+) cells, qualitatively the number of spheroids and the average size of spheroids are increased (**B**). Spheroids mostly comprise cells with strong eGFP fluorescence. **C,D)** Data analyses from 2D-scratch assays with ZL55-SO cells. **C)** The mobility in the direction of the wound closure zone (empty space) between eGFP(+) (green trace) and eGFP(-) cells (black trace) is not different. A phase of higher mobility lasting for less than 2 h is followed by a phase of approximately 12 h characterized by a constant lower mobility of all cells. Dotted lines represent standard deviations. **D)** The non-directed movement of ZL55-SO cells at low confluence (<10%) shows no differences between eGFP(+) (green solid line) and eGFP(-) cells (black solid line). Traces represent the average shift of 10 randomly selected cells. **E,F)** Merged fluorescent and brightfield images of untreated MSTO-211H-SO cells containing approximately 5% of eGFP(+) cells **(E)** and NF2-overexpressing MSTO-211H-SO cells 84 h post-transfection **(F)** NF2 expression causes massive cell death and essentially all surviving cells derive from the subpopulation of eGFP(+) cells. **G-J)** All growth curves are from one selected real-time experiment, but are representative for at least 3-4 independent experiments for all cell types. Dotted lines represent standard deviations. **G)** NF2 overexpression decreases proliferation of murine RN5-SO cells, but much less of puromycin-selected (eGFP(+)) RN5-SO-P2 cells. **G-I)** Similar and even stronger effects are observed in human MM cell lines. **H,I)** NF2 overexpression almost completely blocks cell proliferation of SPC111-SO and ZL5-SO cells (left) compared to only mild effects on proliferation in the eGFP(+) population of SPC111-SO-P2 and ZL5-SO-P2 cells. Error bars represent standard deviations. **J)** NF2 overexpression also strongly decreases proliferation of MSTO-211H-SO cells, but only mildly affects proliferation of MSTO-211H-SO-P2 (eGFP(+)) cells (right).

5

Supplemental movies M1 – M4 (in .mp4 format)

Movie M1. A small cluster of eGFP(+) ZL55-SO cells consisting of a mixed population of green and non-green cells was selected. Note that cell division of an eGFP(+) cell results in a green and a non-green eGFP(-) daughter cell. Both daughter cells further divide and the descendants from the newly generated eGFP(-) cells remain non-green. The green daughter cell gives rise to additional eGFP(+) cells.

Movie M2: Time-lapse series of ZL55-SO-P2 cells maintained in culture *in vitro* for 80 days. Initially all cells are eGFP(+). The movie shows several rounds of passaging and re-plating. With time, the percentage of eGFP(+) cells decreases and the fraction of non-green eGFP(-) cells starts to increase. During each passaging a region within the cell culture dishes was selected that contained at least a fraction of eGFP(+) cells.

Movie M3: Video of ZL55-SO parental cells (mixed population), where the functional human NF2 tumor suppressor was over-expressed. All non-green eGFP(-) cells essentially present on the left half of the video frame) are extremely sensitive to NF2 overexpression; most cells undergo cell death evidenced by the loss of the cell shape and the appearance of cell debris remaining after cell death. At the end of the observation period (>120 h) essentially only eGFP(+) cells remain.

Movie M4: Different behavior of FACS-sorted ZL55-SO^{high} cells, initially consisting of 100% eGFP(+) cells. ZL55-SO^{high} cells that have lost eGFP expression over time resulting in eGFP(-) cells. Initially eGFP(+) cells maintained without puromycin selection for 7 weeks were transduced with the lentiviral construct LV-NF2. NF2 overexpression induced apoptosis selectively in eGFP(-) cells, while eGFP(+) cells were not affected by increases in NF2. This supports the hypothesis of a functional differentiation from eGFP(+) to eGFP(-) cells and not a mere down-regulation of eGFP expression resulting from e.g. a promoter-silencing artifact such as hypermethylation of the lentiviral plasmid promoter region.

Supplemental Experimental Procedures

Cell culture and selection of SOX2/OCT4-expressing cells

The human mesothelioma cell lines ZL55, ZL5, SPC111 (Schmitter et al., 1992), MSTO-211H and the murine mesothelioma cell line RN5 (Blum et al., 2015b) were maintained in RPMI1640 (Gibco, Basel, Switzerland) supplemented with 10% fetal bovine serum (FBS; Gibco), 100 U/ml penicillin and 100 mg/ml streptomycin (1% PS). Mesothelioma cell lines were transduced with lentivirus containing the SOX2/OCT4 stemness indicator construct pL-SIN-EOS-S(4+)-EiP (Hotta et al., 2009a; 2009b); cell lines containing the stemness indicator construct are named as "*cell line name*-SO". A variable fraction of cells in each cell line expressed the enhanced green protein eGFP forming the eGFP(+) population, while the other non-fluorescent cells comprise the eGFP(-) population. This allows for the identification and the selection of high SOX2- and OCT4-expressing (SO) CSC-enriched cells based on endogenous SOX2 and OCT4 expression levels sufficient to drive eGFP expression. In few experiments cells were transduced with a lentiviral reporter construct in which six concatenated repeats of a composite SOX2/OCT4 response element (SORE6) had previously allowed to obtaining a breast cancer cell population enriched in CSC (Tang et al., 2015). In some experiments, eGFP(+) cells were selected with either 2 µg/ml (-SO-P2 cells) or 10 µg/ml (-SO-P10 cells) puromycin (Sigma-Aldrich, Buchs, Switzerland) for either 10 days or in some cases for 3 weeks. In the latter experiments, the selection pressure was then removed and cells cultivated for 10 passages (3 weeks).

Lentiviral constructs, vector production and lentivirus isolation

pL-SIN-EOS-S(4+)-EiP was obtained from Addgene (plasmid #21314) as described in Hotta et al. (Hotta et al., 2009a). Lentivirus coding for pL-SIN-EOS-S(4+)-EiP, for shRNA eGFP and CALB2 were produced and isolated as described before (Blum and Schwaller, 2013). The plasmid CSCW2-NF2 was a kind gift of Prof. J.F. Gusella (James et al., 2008) and the SORE6 reporter plasmid from Dr. L.M. Wakefield (Tang et al., 2015). The GFP cassette in pLVTHM (Addgene plasmid #12247; (Wiznerowicz and Trono, 2003)) was replaced with a mCherry-NLS fragment. Briefly, the plasmid mCherry-NLS (gift from Martin Offterdinger (Addgene plasmid # 39319; (Micutkova et al., 2012) was digested with *AgeI*, filled with Klenow enzyme, and then digested with *XbaI*. The insert was ligated into pLVTHM using the compatible *PmeI* and *SpeI* sites. Lentivirus was produced by the calcium phosphate transfection method using HEK293T as described before (Blum and Schwaller, 2013).

Treatment of cells with cis-Pt, 5-fluorouracyl (5-FU) and the focal adhesion kinase (FAK) inhibitor VS-6063 and determination of IC$_{50}$ values

Cells were seeded in 96-well plates (500 cells per well) and grown for 24h. Cis-Pt (Sigma-Aldrich, Buchs, Switzerland) was added in a concentration range from 0.625 to 10 mM and the MTT assay was performed either 96h or 120h post treatment to determine the number of viable and/or proliferating cells (Marilley et al., 2001). Real-time cell proliferation curves and images were acquired with the Incucyte Live-cell imaging system (Essen Bioscience, Ann Arbor, MI) as described before (Blum et al., 2015a). For the VS-6063 toxicity assays, cells were seeded in 96-well plates (2,000 cells per well) and grown for 24h. VS-6063 (Selleckchem, Houston, USA) was added in a concentration range from 2.5 to 10 mM and the MTT assay was performed after 48h. 5-FU (Sigma-Aldrich, Buchs, Switzerland) was added in a concentration range from 0 to 100 mM and the MTT assay was performed after 48h. IC$_{50}$ values were calculated using Graphpad Prism 7 (Graphpad Software, CA, USA) by fitting on normalized data.

Flow cytometry analysis of eGFP(+) cells

Sub-confluent cultured MM cells were trypsinized; cell pellets were collected and washed three times with PBS before re-suspension in PBS. Flow cytometry was performed on a BD Accuri C6 (BD Biosciences) for eGFP expression and data were analyzed with the FlowJo software (Tree Star). Sorting of eGFP-expressing cells (ZL55-SO^{high} and RN5-SO^{high} vs. ZL55-SO^{low} and RN5-SO^{low}) was performed on a BD FACS ARIA (BD Biosciences) cell sorter (100 µm nozzle, 20 psi) and selected for subsequent cell culture *in vitro*.

Determination of stemness genes mRNA expression levels by quantitative real-time PCR

To investigate the quantitative mRNA expression of *SOX2*, *OCT4*, *ABCG2* and *CSF1R*, total RNA was extracted from 80% confluent cell cultures of ZL55-SO-P0/P2/P10 cells (6-wells) following the manufacturer's instructions (PeqGold TriFast^{TM}). Reverse transcriptase and qRT-PCR were performed using Qiagen kits. qRT-PCR primer sequences for *SOX2*, *OCT4* and *CSF1R* were reported before (Cioce et al., 2014) as were the ones for *ABCG2* (Frei et al., 2011) and for the control ribosomal

protein S13 (*RPS13*). The primer sequences for *KLF4* and *c-Myc* were taken from (Pasdar et al., 2015), for mNanog, mSox2 and mOct4 from (Chen et al., 2006), for Rbs23 from (Henzi and Schwaller, 2014).

Primer sequences used for RT-PCR

Genes		Primer sequence 5'– 3'
ALDH1A1	F	CTG CTG GCG ACA ATG GAG T
	R	GTC AGC CCA ACC TGC ACA G
KLF4	F	CTG GGT CTT GAG GAA GTG CT
	R	GGC ATG AGC TCT TGG TAA TGG
c-Myc	F	GGA CTT GTT GCG GAA ACG AC
	R	CTC AGC CAA GGT TGT GAG GT
UBC	F	GAT TTG GGT CGC GGT TCT T
	R	TGC CTT GAC ATT CTC GAT GGT
mNanog	F	AGG GTC TGC TAC TGA GAT GCT CTG
	R	CAA CCA CTG GTT TTT CTG CCA CCG
mOct4	F	CTG TAG GGA GGG CTT CGG GCA CTT
	R	CTG AGG GCC AGG CAG GAG CAC GAG
mSox2	F	GGC AGC TAC AGC ATG ATG CAG GAG C
	R	CTG GTC ATG GAG TTG TAC TGC AGG
mRps23	F	ATG CCT TGT GGG TCC TTC CTG C
	R	ACG ACA CTT GCC CAT CTT GCC GG
RPS23	F	CGA AAG CAT CTT GAG AGG AAC A
	R	TCG AGC CAA ACG GTG AAT C

Western blot assays for calretinin, NF2 and mesothelin
Cells were seeded into 25 cm^2 flasks (TPP, Trasadingen, Switzerland) and harvested at 70-90% confluence. Proteins were extracted from washed cell pellets using standard RIPA buffer (50 mM Tris, 150 mM NaCl, 0.1% sodium dodecyl sulfate (SDS), 0.5% sodium deoxycholate, 1% Triton X-100, pH 7.4). Samples were incubated 5 min on ice, centrifuged for 15 min (14,000 x g, 4°C) and the supernatant was collected. Proteins (50 μg) were separated on 10% polyacrylamide SDS gels and transferred onto nitrocellulose membranes. Loading was controlled using Ponceau S staining and membranes were blocked with 5% milk in 0.1% Tween 20 in PBS for 1h at room temperature and incubated overnight at 4°C with primary antibodies: Calretinin CR7699/4: dilution 1:10,000 (SWANT, Marly, Switzerland); Mesothelin: dilution 1:2,000 (clone B-3, Santa Cruz Biotechnology, Santa Cruz, CA); NF2 A-19: dilution 1:1,000; Santa Cruz). Secondary biotinylated antibodies were added at a dilution of 1:10,000 for 2h at room temperature and incubated for 30 min with the ABC system (Vectastain, Vector Laboratories, Burlingame, CA). The HRP substrate (Millipore, Luminata Forte) was applied to the membrane for 3 min and membranes were imaged on the Western Blot reader FluorChem E System (Bucher Biotec, Basel, Switzerland).

Spheroid formation
MSTO-211H cells (obtained from ATCC) were transduce with the –SO reporter construct and maintained under standard conditions (RPMI, 1% PS, 10% FBS) and seeded (50,000 cells/well) in 6-

well plates in serum-free growth conditions. Spheroid formation of MSTO-211H-SO and MSTO-211H-SO-P2 cells was monitored with the Incucyte Live-Cell imaging system and images were taken every hour.

Limiting Dilution Assay *in vitro*
Limiting dilution assays *in vitro* were performed as described before (Thiagarajan et al., 2015; Wiechert et al., 2016). Briefly, MM cells were seeded in serial dilutions (1-20 cells/well) with 100 μL serum-free DMEM/F12 medium supplemented with 10 ng/ml epidermal growth factor (Sigma, Switzerland), 20 ng/ml basic fibroblast growth factor (Thermofisher, Switzerland), 10 μg/ml insulin (Sigma, Switzerland) and 2% B27 (Thermofisher, Switzerland). The frequency of sphere formation was calculated as described before (Thiagarajan et al., 2015; Wiechert et al., 2016); a well with a tumor sphere was counted as a positive well (1) and a well without a tumor sphere as negative (0). 2 weeks after seeding of the cells the tumor spheres were counted under a phase contrast microscope (n = 3 independent experiments).

Soft Agar Assay
The assay was performed as described previously (Blum et al., 2015b; Provost et al., 2012). In a microwave oven 1% agar was melted in RPMI and mixed with pre-warmed 2x RPMI completed with 20% FCS and penicillin-streptomycin to prepare the 0.5% base agar. The base agar (1 ml) was poured into 6-well plates and set aside to solidify. In a microwave oven 0.7% of agarose was melted and mixed with equal volumes of 2x RPMI with 20% FCS. The medium was allowed to cool down and cells were added (5,000 cells/well in 6-well plates). Plates were incubated for 2 weeks and twice per week the wells were supplied with 0.5 ml of fresh culture medium. The area (2D) of the spheroids on the acquired images was quantified using the Fiji software. From the measured area assuming to be a perfect circle, the circle's radius, was calculated. We presumed that this would also correspond to the radius of a perfect spheroid. The area of a circle is equal to $\pi \times r^2$; reported values correspond to the calculated radii (mean±SEM).

Cell tracking
ZL55-SO cells were transduced with lentivirus containing pLV-mCherry-NLS coding for a fusion protein consisting of the mCherry red fluorescent protein fused to a nuclear localization signal (NLS). ZL55-SO cells (10,000-20,000) were plated in 96-well plates and 24 h after plating, a scratch of about 1 mm was created using the Wound Maker tool (Essen Bioscience) and the cell culture medium was replaced. The scratch area was monitored every 15 min using a Leica DMI6000B microscope equipped with a CO_2/temperature-conditioned incubator. To assess the cell motility, the movements of the cells migrating primarily towards the center of the scratch were recorded. For the image analysis a Java ImageJ plugin (CGE) was used (http://bigwww.epfl.ch/sage/soft/circadian/) that had been developed for tracking cells in the context of circadian studies (Sage et al., 2010).

Supplemental References

Chen, S., Do, J.T., Zhang, Q., Yao, S., Yan, F., Peters, E.C., Schöler, H.R., Schultz, P.G., Ding, S., 2006. Self-renewal of embryonic stem cells by a small molecule. Proc. Natl. Acad. Sci. U.S.A. 103, 17266–17271.

Cioce, M., Canino, C., Goparaju, C., Yang, H., Carbone, M., Pass, H.I., 2014. Autocrine CSF-1R signaling drives mesothelioma chemoresistance via AKT activation. Cell Death and Disease 5, e1167–11.

Henzi, T., Schwaller, B., 2014. Antagonistic Regulation of Parvalbumin Expression and Mitochondrial Calcium Handling Capacity in Renal Epithelial Cells. PLoS ONE 10, e0142005–e0142005.

Hotta, A., Cheung, A.Y.L., Farra, N., Vijayaragavan, K., Séguin, C.A., Draper, J.S., Pasceri, P., Maksakova, I.A., Mager, D.L., Rossant, J., Bhatia, M., Ellis, J., 2009b. Isolation of human iPS cells using EOS lentiviral vectors to select for pluripotency. Nature Methods 6, 370–376.

James, M.F., Lelke, J.M., MacCollin, M., Plotkin, S.R., Stemmer-Rachamimov, A.O., Ramesh, V., Gusella, J.F., 2008. Modeling NF2 with human arachnoidal and meningioma cell culture systems: NF2 silencing reflects the benign character of tumor growth. Neurobiology of Disease 29, 278–292.

Marilley, D., Vonlanthen, S., Gioria, A., Schwaller, B., 2001. Calretinin and calretinin-22k increase resistance toward sodium butyrate-induced differentiation in CaCo-2 colon adenocarcinoma cells. Experimental Cell Research 268, 93–103.

Micutkova, L., Hermann, M., Offterdinger, M., Hess, M.W., Matscheski, A., Pircher, H., Mück, C., Ebner, H.-L., Laich, A., Ferrando-May, E., Zwerschke, W., Huber, L.A., Jansen-Dürr, P., 2012. Analysis of the cellular uptake and nuclear delivery of insulin-like growth factor binding protein-3 in human osteosarcoma cells. Int. J. Cancer 130, 1544–1557.

Provost, J.J., Rastedt, D., Canine, J., Ngyuen, T., Haak, A., Kutz, C., Berthelsen, N., Slusser, A., Anderson, K., Dorsam, G., Wallert, M.A., 2012. Urokinase plasminogen activator receptor induced non-small cell lung cancer invasion and metastasis requires NHE1 transporter expression and transport activity. Cell Oncol. 35, 95–110.

Sage, D., Unser, M., Salmon, P., Dibner, C., 2010. A software solution for recording circadian oscillator features in time-lapse live cell microscopy. Cell Div 5, 17.

Schmitter, D., Lauber, B., Fagg, B., Stahel, R.A., 1992. Hematopoietic growth factors secreted by seven human pleural mesothelioma cell lines: interleukin-6 production as a common feature. Int. J. Cancer 51, 296–301.

Wiznerowicz, M., Trono, D., 2003. Conditional suppression of cellular genes: lentivirus vector-mediated drug-inducible RNA interference. Journal of Virology 77, 8957–8961.